Indian Journal of Biochemistry & Biophysics
Vol. 62, August 2025, pp. 935-947
DOI: 10.56042/ijbb.v62i8.17039

HMG-CoA Reductase inhibition targeted hypercholesterolemic potential of phytoconstituents of an aqueous shoot extract of *Calligonum polygonoides* L.: Insight from *in vitro, in vivo* and *in silico* assessments

Anita Sakarwal[1], Karishma Sen[1], Heera Ram[1]*, Pushpa Potaliya[2], Jaykaran Charan[3], Mukesh Kumar Yadav[4] & Anil Panwar[5]

[1]Department of Zoology, Jai Narain Vyas University, Jodhpur-342 011, Rajasthan, India

[2]Department of Anatomy; & [3]Department of Pharmacology, All India Institute of Medical Sciences, Jodhpur-342 005, Rajasthan, India

[4]Department of Microbiology, Central University of Punjab, Bhatinda-151 401, Punjab, India

[5]Department of Bioinformatics and Computational Biology, CCS Haryana Agricultural University, Hisar-125 004, Haryana, India

Received 10 February 2025; *revised 06 May 2025*

Calligonum polygonoides L. is a desertic plant used for the therapeutics of several metabolic disorders and ethnomedicines. Current study was assigned to examine the 3-hydroxy-3-methylglutaryl coenzyme A (HMG-CoA) reductase inhibition targeted hypocholesterolemic potential of *Calligonum polygonoides* L. through *in silico, in vitro* and *in vivo* assessments. The LC-MS/MS screening of the aqueous shoot extract showed leading compounds and structural data retrieved from an authentic repository of PubChem. The interactions of HMG-CoA reductase (HMGR) and ligands complex were examined using molecular docking. Significant interaction was shown by dihydrocelastrol with the target enzyme (HMGCR) up to a binding energy of -8.9 Kcal/mol. The assessments of Root Mean Square Deviation, Root Mean Square Fluctuation, radius of gyration, and Solvent Accessible Surface Area along with Molecular Mechanics - Poisson-Boltzmann Surface Area and PCA were examined by GROMACS 2020.2 of best-docked complexes at 100 ns with standards. Consequently, the competent HMGCR inhibition performed by the test extracts up to 75.8% (IC_{50} = 219.5 µM) through *in vitro* assessments. Encouragingly, the treatment of test extract showed significant reductions in lipid profile, dyslipidemia indices, and glucose level along with ameliorations in oxidative stress. Subsequently, significant restorations were revealed in the arterial wall of the coronary arteries. Based on the results, it can be concluded that dihydrocelastrol is a potent bioactive phytocompound that can inhibit the HMGCR and significantly reduce hypercholesterolemia.

Keywords: *Calligonum polygonoides* extract, Druggability, HMG-CoA reductase, Hypercholesterolemia, Masson trichome

Conventional hypocholesterolemic formulations are composed of potent small molecule phytocompounds that target the key enzymes of cholesterol biosynthesis and ameliorations the oxidative stress[1,2]. Accordingly, the statins subside to the biosynthesis of cholesterol through inhibition of HMG-CoA (3-hydroxy-3-methylglutaryl coenzyme-A) reductase (at the rate-limiting stage in cholesterol biosynthesis)[3]. The reduced intracellular cholesterol convinces the expression of the low-density lipoprotein receptor (LDLR) and increases the uptake of LDL from the blood, with a concomitant decrease of plasma concentrations of LDL-cholesterol (LDL-C). Accordingly, the numerous small molecule phytocompounds obtained fromlocal plants possess capabilities to inhibit the HMGCR and ameliorations in oxidative stress.

Correspondence:
E-mail: hr.zo@jnvu.edu.in, baradhr@gmail.com

The *Calligonum polygonoides* L. is a regional plant of the Thar desert and is reported for numerous ethnomedicinal uses with a track record of local practices in diet and ethnomedicines[4,5]. Locally, *C. polygonoides* has been utilized as a potent herbal remedy for several ailments such as an antidote against snake bites, heavy doses of opium, curing typhoid, asthma, cough and cold[6].The different parts of *C. polygonoides* such as flower bud and shut epical parts are also used in specific local food recipes as per the long practices and knowledge transmission from the next generations. The desert-inhabitant plants are rich sources of secondary metabolites and stress-raised bioactive small molecule phytocompounds which are common ingredients of conventional formulations[6,7]. Subsequently, previous studies reported the occurrence of different secondary metabolites in different parts of *C. polygonoides*, specifically phenolics, flavonoids, tannin, steroids, and terpenoids, and exhibited its higher scavenging

activity against DPPH, ABTS, and superoxides along with anti-fungal and cytotoxicity against *Aspergillus niger* and brine shrimp, respectively.

In this study, we sought to investigate the HMGCR inhibition potential of small molecule phytocompounds of *Calligonum polygonoides* L. aqueous extracts.

Materials and Methods

Chemicals and reagents

Poloxomer407 and cholesterol powder were purchased from Sigma (St. Louis, USA) through a local distributor. Other chemicals and reagents used were of analytical grade purchased from Sigma (St. Louis, USA). Atorvastatin was purchased from the registered pharma distributor (Pharma Agency Healthcare Limited, Jodhpur, Rajasthan, India).

Selected plant material

During the months of September and October 2021, shoots of *Calligonum polygonoides* L. were collected from the surrounding region of Karlu, Nagour district, Rajasthan, India. The collected plant material was authenticated by the taxonomist and the specimen has been deposited at the herbarium of the regional centre of Botanical Survey of India, Jodhpur by issuing the voucher (No: BSI/AZRC/I.2012/ Tech./2022-23 (PI. -ID.)/142).

Extract preparation

The dried shoots were powdered and proceeded for extract preparation with a packed filter paper pouch and kept under the aqueous solution. The soxhlation of the extract was followed under standard temperature and duration up to the cleaning of the material[9]. The obtained extract proceeded through the gradual evaporation and vacuum-dried.

Phytochemical analysis by LC-MS/MS

The plant extract was examined through the LC-MS/MS (liquid chromatography-tandem mass spectrometry) under the standard acquisition conditions by negative and positive ionizations for the screening of the exhibited small molecule phytocompounds[10]. The exhibited small molecule phytocompounds were identified through the resemblances of molecular weight, retention time, and mz values from the authorized chemical library by authenticated software.

In vitro HMGCR assay

The HMG-CoA reductase (HMGCR) inhibition potential of the test extract and atorvastatin (Standard drug) was examined by using the commercially available diagnostic kit (Sigma Aldrich). The inhibition potential was calculated based on a spectrophotometric measurement of the decrease in absorbance, which revealed the oxidation of NADPH by the catalytic subunit of HMGR in the occurrence of the substrate HMG-CoA. The ascending concentrations of test extract and Atorvastatin were obtained for the assessments of the HMGCR inhibition capabilities through calculations of IC_{50} and enzyme kinetics[11,12].

Chemical hypercholesterolemia induction method by poloxamer 407

The hypercholesterolemia was induced through intraperitoneal administration of poloxamer-407 (at a concentration of 500 mg/kg each week)[13,14]. Poloxamer was dissolved in a buffer isotonic solution and administered intraperitoneally for the duration of four weeks. Animals were fed with high-fat diet and monitored for lipid metabolic status. The hypercholesterolemia was confirmed by the assessments of lipid profile and dyslipidemia indices.

In vivo evaluation of hypercholesterolemia inhibition

Adult male albino rats were selected for animal models of hypercholesterolemia weighing 200-250 g. The experimental animals were divided into four groups, where each group consisted of five animals. Experimental animals were kept in controlled environmental conditions with optimum temperature (22-26°C) and a 12 h light cycle by following the recommendations of CPCSEA. The protocol (IAEC No: JNVU/IAEC/2020/02) was approved and recommended by the IAEC (Institutional Animal Ethical Committee). Experimental groups were designed to be as follows:

Group I: Intact vehicle control
Group II: Hypercholesterolemia control
Group III: Treatment of shoot aqueous extract of *Calligonum polygonoides* L.
Group IV: Treatment of atorvastatin

Dose and duration of experiments

The experimental animals were fed on the doses of 20 mg/kg of atorvastatin[15]and 400 mg of the extract[16,17]for four weeks. The doses of test extract and atorvastatin were administered using a suitable solvent (distilled water and buffer).

Biochemical analysis

Overnight fasted animals were autopsied under mild anaesthesia and proceeded for the serum

biochemistry assessments using available diagnostic commercial kits.

Serum lipid profile and atherogenic index

Total cholesterol[18], HDL-cholesterol[19], and triglycerides[20] were measured by following the standard methods and calculated the lipid profile by using Friedewald's formula[21].

Ldl-cholesterol = Total Cholesterol - HDL-cholesterol – VLDL-cholesterol

Where VLDL = TG/5

The Castelli risk index-I (Total cholesterol /HDL), Castelli risk index-II (LDL/HDL), and the Atherogenic index = Log (triglyceride/HDL-cholesterol) were calculated by using this formula and prescribed protocols[22,23].

Assessments of oxidative stress

The oxidative stress was measured by following the assessments of lipid peroxidation (LPO)[24], glutathione (GSH)[25], and ferric-reducing antioxidant potential (FRAP)[26] were estimated by using the standard protocols. Antioxidants were calculated and compared with the standard protocols from different experimental groups.

Histological studies

Ventricular muscles were collected from the heart and fixed in 10% formalin. The fixed tissues were proceeded through sequential steps of dehydration, clearing, and embedded in paraffin wax for the block preparations. Ventricular tissues embedded block proceeded for the sectioning at 5µ and followed Masson's trichome staining.

Masson trichrome staining for coronary arteries

Trichrome stains, such as Masson's Trichrome, are a type of histological staining technique that employs three dyes to selectively stain different tissue components[27]. These stains utilize acid-base chemistry to target specific structures, such as muscle, collagen fibers, fibrin, and erythrocytes. Accordingly, the selected ventricular tissues followed the standard protocol of this kind of trichrome staining (Masson's trichrome) and were examined for the assigned objective. The collagen-positive area was quantified using the ImageJ software.

***In silico* studies**

The *in silico* assessments were performed by following the molecular docking, molecular dynamics, and Absorption, Distribution, Metabolism, and Excretion-Toxicity (ADMET).

Molecular docking using AutodockVina

Protein-ligand molecular docking was performed by the retrieved data from Protein data bank (PDB) for the target protein and ligand from PubChem[28]. The data of ligand and target proteins were proceeded for the preparation of autodock run. The complex grids were analyzed and prepared as per standard parameters. The results of autodock were examined for the binding energies, H bonding, availabilities of pi ponds, and relative interactive forces.

Molecular dynamic stimulation studies

To gain insight into the behavior of best-docked complexes, MD simulations were performed using the GROMACS 2020.2 package[29,30]. The best-docked complexes, *i.e*., dihydrocelastrol and Atorvastatin with 1DQA were studied. Receptor topologies were created using GROMACS's pdb2gmx module. Additionally, the topology of the ligands was generated separately using SwissParam, an automated server. Proteins were positioned at least 1.0 nm from the box's edges while systems were solvated using a dodecahedron box. Energy minimization was performed after adding the required charges to the system. Potential energy was minimized at a maximum force of 1000.0 KJ/mol/nm with a cut-off of 50, 000 energy minimization steps. The temperature coupling was carried out by treating the protein structure and ligand as a single entity for 100ps at 310K while saving the complex coordinates every 10ps. Parrinello-Rahman pressure coupling was also used to achieve the pressure equilibrium. Systems were then subjected to a 100 ns molecular dynamics simulation to check the stability of the complexes. The Radius of Gyration (Rg), Solvent accessible surface area (SASA), Root Mean Square Deviation (RMSD), and Root Mean Square Fluctuations (RMSF) were used for structural analysis. The Molecular Mechanics Poisson-Boltzmann Surface Area (MMPBSA) approach was also used to calculate the free energies of protein-ligand binding interactions. The principal component analysis (PCA) was also carried out. The graphs were generated using xm-grace.

ADMET and BOILED egg assessments

ADMET Predictor is a machine learning software tool that assesses the druggability assessments by

following the records of repositories and characteristics of the standard drug molecule[31]. This kind of software provides the data of significant values of solubility, logP, pKa, sites of CYP metabolism, mutagenicity, and major PK endpoints using integrated Drulito software. The most well-known rule-based filter for determining whether a substance is well absorbed orally is the Rule of Five, also known as the Lipinski Rule of Five. It is a set of four ADMET properties that include Molecular weight<500 M; iLOGP< 5 octanol/water partition coefficient a total of 5 hydrogen bond donors (HBDs), and a total of 10 hydrogen bond acceptors (HBAs)[19]. The gastrointestinal absorption was examined by BOILED egg assessment by following the standard parameters[32].

Statistical analysis

The statistical significance was detected by one-way ANOVA and variances, and the P value less than 0.05 was considered significance.

Results

Screening of phytoconstituents by LCMS

Data retrieved from LC-MS/MS of test extract (aqueous shoot extract of *Calligonum polygonoides* L.) were examined throughan existing chemical library of MEDLINE. Data was analyzed based on QTOF mass hunter software following the parameters of the monoisotopic mass, mz values, and time of retention. The examination of the test extract shown existence of leading 17 phytoconstituents such as sparteine, D-Glucuronic acid 1-phosphate, Indican 12Z, 15S, 18S) -15-hydroxy-18-bromo-12, 16, 17-octadecatrienoic acid, Nobiletin, Khelloside, Vismione D, Hecogenin, Methyl 2, 6-dihydroxy-4-quinolinecarboxylate, Dihydrocel astrol, Convallagenin B, Vitisin B, Sativanine B, Prunus inhibitor b, 5, 4'-Dihydroxy-6-C-prenylflavanone 4'-xylosyl- (1->2) -rhamnoside, Linoside B, (R) -Skyrin 2-xyloside andLicorice glycoside E (Table 1).

Inhibition of HMG-Co A reductase activity *in vitro* assay

The inhibitory effect of the aqueous shoot extract of *Calligonum polygonoides* L. as compared to the positive control (atorvastatin, a standard drug) was determined at various concentrations by following the ascending concentrations against the product complex molecule. Aqueous extract showed 75.8% inhibition as compared to atorvastatin which showed 80.01% inhibition. Using, the online AAT Bioquest calculator,

Table 1 — Identified masses from UPLC-QTOF mass spectroscopy constituents in an aqueous extract of *Calligonum polygonoides* L. string with monoisotopic mass and METLIN ID.

S.N.	Identified compound name	Formula	Monoisotopic mass (g/mol)	Metline ID	ΔPPM	CAS
1	5, 4'-Dihydroxy-6-C-prenylflavanone 4'-xylosyl- (1->2) -rhamnoside	$C_{31}H_{38}O_{12}$	602.23	52591	8	-
2	12Z, 15S, 18S) -15-hydroxy-18-bromo-12, 16, 17-octadecatrienoic acid	$C_{18}H_{29}BrO_3$	372.13	96820	1	-
3	Convallagenin B	$C_{27}H_{44}O_6$	464.31	84192	6	-
4	D-Glucuronic acid 1-phosphate	$C_6H_{11}O_{10}P$	274.00	58195	6	13168-11-1
5	Dihydrocelastrol	$C_{29}H_{40}O_4$	452.29	44189	0	-
6	Hecogenin	$C_{27}H_{42}O_4$	430.30	43920	5	467-55-0
7	Indican	$C_{14}H_{17}NO_6$	295.10	524	5	487-60-5
8	Khelloside	C19H20O10	408.10	67349	4	17226-75-4
9	Linoside B	$C_{30}H_{36}O_{15}$	636.20	49486	2	-
10	Loganin pentaacetate	$C_{27}H_{36}O_{15}$	600.20	41175	3	-
11	Methyl 2, 6-dihydroxy-4-quinolinecarboxylate	$C_{11}H_9NO_4$	219.05	93963	2	66416-75-9
12	Nobiletin	$C_{21}H_{22}O_8$	402.13	44436	1	478-01-3
13	Prunus inhibitor b	$C_{30}H_{24}O_{11}$	560.13	92515	2	83889-81-0
14	Sativanine B	$C_{30}H_{38}N_4O_4$	518.28	68092	6	72361-60-5
15	(R) -Skyrin 2-xyloside	$C_{35}H_{26}O_{14}$	670.13	91464	2	-
16	Sparteine	$C_{15}H_{26}N_2$	234.38	44021	9	-
17	Vismione D	$C_{25}H_{30}O_5$	410.20	68060	5	87605-72-9
18	Licorice glycoside E	C35H35NO14	693.2058	52522	2	-

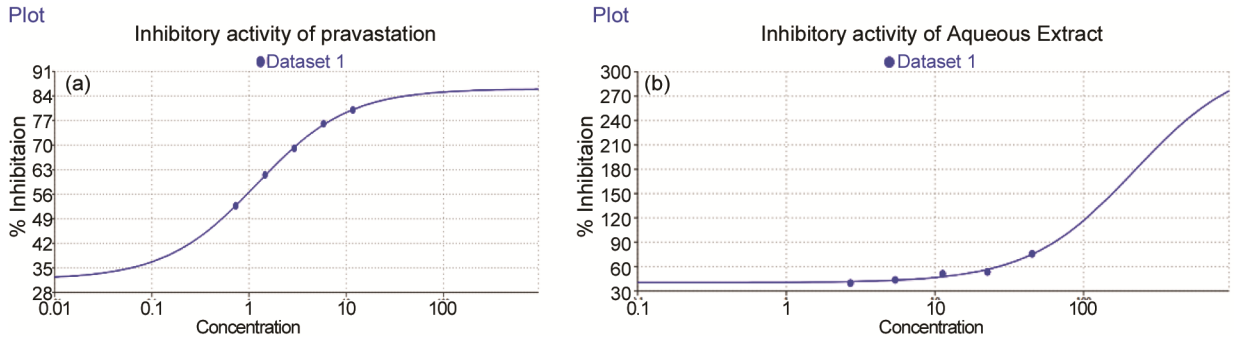

Fig. 1 — A.) *In vitro* inhibitory activity of Atorvastatin as positive control against HMGCR enzyme. (IC_{50} = 1.2019nM). B.) *In vitro* inhibitory activity of Aqueous extract of *Calligonum polygonoides* L. strig against HMGCR enzyme. (IC_{50} = 219.5µM).

the IC_{50} values for string extract and atorvastatin were determined to be 219.5 and 1.2019, respectively, (Fig. 1A & B).

Assessments of lipid profile and dyslipidemia indices

The induction of poloxamer 407 and high-fat diet caused significant alterations in total cholesterol, triglyceride (TG), LDL (Low-density lipoprotein), VLDL (Very low-density lipoprotein) , and HDL (High-Density Lipoprotein) in comparison to the control groups. The treatment of test extract caused significant ($P \leq$ 0.001) ameliorations in hypercholesteremia (Fig. 2A).

Consequently, the dyslipidemia indices *i.e.*, Castelli index I, Castelli index II, atherogenic coefficient, and atherogenic plasma index (AIP) were improved in contrast to ameliorations in lipid profile through the treatment of the test extract (Fig. 2B).

Ameliorations in oxidative stress

Aberrant and variable levels of GSH (Glutathione) and LPO (Lipid Peroxidation) along with total antioxidant levels were observed in the hypercholesterolemia which represented the oxidative stress and degenerative changes. The treatments (Test extract and atorvastatin) caused significant ameliorations in oxidative stress through improved levels of GSH (Glutathione) and LPO (Lipid Peroxidation) (Fig. 3A). Subsequently, the treatments also caused significant moderations in total antioxidant levels through alterations in FRAP values (Fig. 3B).

Histology of the coronary artery

The histology of the coronary artery shows the composition of three layers such as intima, media, and adventitia along with the distribution of different endothelium, elastin, fibrin, and blood vessels.

The stained tissues revealed blue coloration for the connective tissue, nuclei were stained to dark purple,

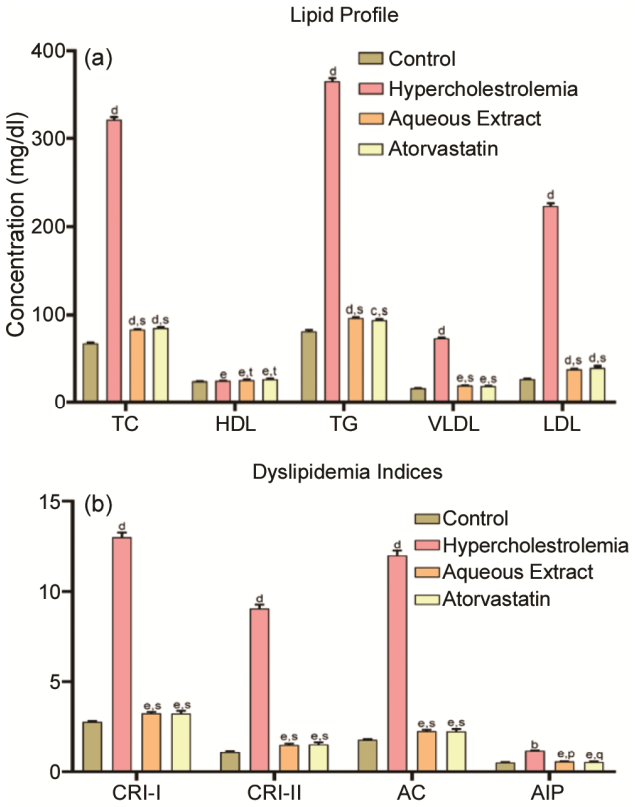

Fig. 2A — Alterations in Lipid profile in poloxamer induce hyperlipidemia rats through treatment of *Calligonum polygonoides* L. aqueous Mean of five values ± SEM. Data are means ± SD (n = 5); Statistical analysis was done using two-way ANOVA. a, b, c, d were significant with *P* value of ≤ 0.1, ≤0.01, ≤ 0.001, ≤0.0001 for the control group; p, q, r, s were significant with *P* value of ≤ 0.1, ≤0.01, ≤ 0.001, ≤0.0001 for the diabetic group and e and t were non-significant as compared to the respective groups. P significant value was ≤ 0.05.

cytoplasm stained to pink, and elastin tissues stained to yellow in the coronary wall of vehicle control whereas the hypercholesterolemia showed abrupt histoarchitectures (Fig. 4A & B). Consequently, the treatments caused significant restorations in three layers of a wall along with the distribution of the

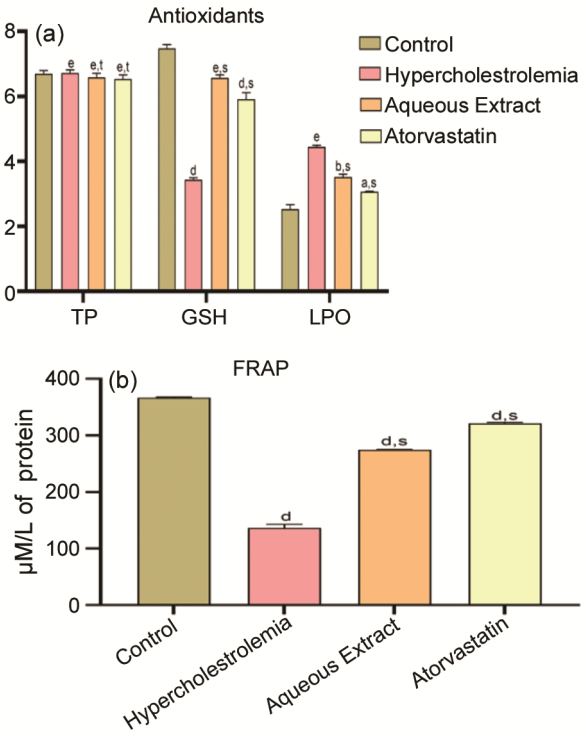

Fig. 3 — (A) Alterations in Antioxidants in poloxomer induce hyperlipidemia rats through treatment of *Calligonum polygonoides* L. aqueous Mean of five values ± SEM. Data are means ± SD (n = 5) ; Statistical analysis was done using two-way ANOVA. a, b, c, d were significant with *P* value of ≤ 0.1, ≤0.01, ≤ 0.001, ≤0.0001 for the control group; p, q, r, s were significant with *P* value of ≤ 0.1, ≤0.01, ≤ 0.001, ≤0.0001 for the hypercholesterolemia group and e and t were non-significant as compared to the respective groups. P significant value was ≤ 0.05; and (B) Alterations in FRAP in poloxamer 407 induce hyperlipidemia rats through treatment of *Calligonum polygonoides* L. aqueous Mean of five values ± SEM. Data are means ± SD (n = 5); Statistical analysis was done using two-way ANOVA. a, b, c, d were significant with *P* value of ≤ 0.1, ≤0.01, ≤ 0.001, ≤0.0001 for the control group; p, q, r, s were significant with *P* value of ≤ 0.1, ≤0.01, ≤ 0.001, ≤0.0001 for the hypercholesterolemia group and e and t were non-significant as compared to the respective groups. P significant value was ≤ 0.05

connective tissues, endothelial tissues, and elastin fibers (Fig. 4C & D).

In silico evaluations

The in silico assessments were followed by molecular docking, molecular dynamics, ADMET predictions, and gastrointestinal absorption by BOILED egg assessment.

Molecular docking

The protein-ligand molecular docking was performed by following the standard parameters. A significant binding energy was shown by the dihydrocelastrol (-8.9 kcal/mol) along with the assessments of H bond availability, access the Lipinski's rules and related assessments dihydrocelastrol was observed in comparison to the standard drug (atorvastatin) (Table 2).

Molecular dynamics

Both systems were solvated and checked for electro-neutrality. The dihydrocelastrol system was neutralized by adding chlorine ions described in (Table 3). The volume of boxes, density of systems, solvent molecules added and Fmax steps were also mentioned in (Table 3). The potential energy minimization of Atorvastatin + 1DQA was achieved in 1599 E.M. steps, indicating that the Atorvastatin + 1DQA system was equilibrated faster than dihydrocelastrol + 1DQA. After the NVT and NPT ensemble, proteins were at a dynamic state at 300K and constant pressure. Both the systems were put to MD Simulations for 100 ns each. To study the degree of compactness of protein during simulation, the Radius of gyration (Rg) was calculated for a span of 100 ns. The Rg value of dihydrocelastrol and atorvastatin 1DAQremains constant with a value of 2.75 nm. The Rg value of Aldose reductase with both ligands remains low and stable with a value of 1.9 nm (Fig. 5A). To study the degree of compactness of protein during simulation, the Radius of gyration (Rg) was calculated for a span of 100 ns. Further, the RMSD value was calculated to determine the fluctuations in the 3D structure of Ligands with time. It was observed that the RMSD of dihydrocelastrol remains increasing till 15ns but thereafter remains stable in the active site of 1DQA throughout the simulation with a value around 5.0Å (Fig. 5B). While in the same receptor, RMSD of Atorvastatin remains very low and stable with a value of 1.5 Å. The RMSF per atom was calculated, showing fluctuation throughout the study of all residues. The peak reveals that in the dihydrocelastrol complex, the protein undergoes more fluctuation than the Atorvastatin complex (Fig. 5C). Free energy of solvation for both systems was found between -10 to -40 DGSolv (Table 4). Solvent accessible surface area (SASA) for both systems was calculated. SASA values were recorded between 200-230 nm^2. The SASA value of the dihydrocelastrol complex remains lesser as compared to Atorvastatin (Fig. 5D). Dihydrocelastrol shows lesser interaction energies as compared to Atorvastatin. The Binding free energies of molecules were calculated through the MMPBSA approach. Bond angle, dihedral angle, CMAP, VDWAALS,

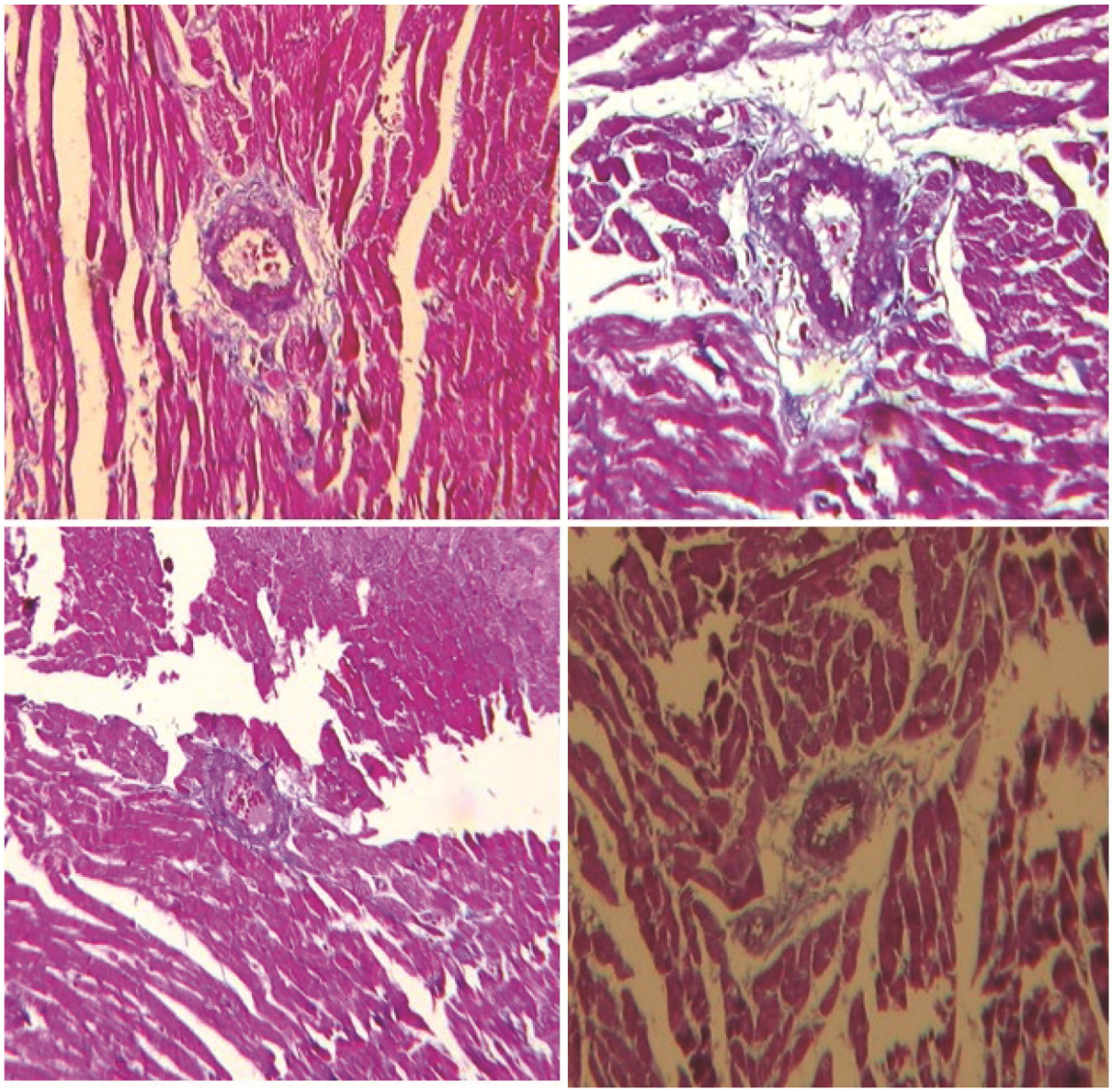

Fig. 4 — Histoarchitecture of heart section of the coronary artery 100 X magnification Masson trichrome staining. (A) Intact control group; (B) Hypercholesterolemia induced group; (C) Aqueous extract treatment; and (D) Treatment with atorvastatin

Table 2 — The binding energies obtained with identified Phyto-compounds of Aqueous extract along with interacting residues and bond length of molecular interaction with 1DQA

S. No	Ligand	Binding Energy (Kcal/mol)	No. of H-bonds	Bond length (Å)	Interacting residues
			Positive control		
1.	Provastatins	-6.7	5	2.06, 2.95, 2.42, (4.41, 2.37)	Ile699, Ile638, Lys606, Lys633
2	Atorvastatin	-7.2	9	(2.15, 4.57) (5.42, 2.98, 3.26) (4.22, 3.95) 4.90, 3.13	Glu610, Lys633, His635, Ala585, Ser705

(*contd.*)

Table 2 — The binding energies obtained with identified Phyto-compounds of Aqueous extract along with interacting residues and bond length of molecular interaction with 1DQA (*contd.*)

S. No	Ligand	Binding Energy (Kcal/mol)	No. of H-bonds	Bond length (Å)	Interacting residues
			Phytoconstituents		
1	5, 4'-Dihydroxy-6-C-prenylflavanone 4'-xylosyl-(1->2) -rhamnoside	-8.2	7	2.04, 2.86, 4.58 (4.56 4.71) 5.09, 2.59.	Leu634, Lys606, Ala585, Pro798, Met742, Gln648.
2.	(12Z, 15S, 18S) -15-hydroxy-18-bromo-12, 16, 17-octadecatrienoic acid	-6.1	9	3.54, (2.71, 2.94) 4.83, 4.91 (4.05, 4.20, 3.5)	Glu700, His635, Lys633, Lys606, Glu610.
3	Convallagenin B	-7.1	4	2.43, (5.28, 4.20) 2.46	Lys633, His635, Glu610.
4.	D-Glucuronic acid 1-phosphate	-6.6	4	(4.52, 2.70) 1.69, 2.19	His635, Lys606, Thr636
5	Dihydrocelastrol	-8.9	3	4.81, 4.56, 2.44	Glu613, Ala585, Thr636.
6	Hecogenin	-8.2	7	(2.51, 2.82) , 2.44, 5.06, 3.73, (5.15, 4.55)	Lys606, His635, Lys633, Thr636, Pro798.
7	Indican	-8.3	6	(2.70, 2.74) 2.13, 1.94, 2.66, 4.36, 3.22.	Glu610, Thr636, Lys606, Ile699, Pro798, Ile638.
8	Khelloside	-7.9	8	(2.38, 2.86) (4.35, 2.16) 3.44, 2.06, 5.00, 4.10.	Lys633, Lys606, Thr636, His635, Trp698, Ala585, Glu610.
9	Linoside B	-7.9	17	2.23, 2.42, (4.82, 5.33) 2.94, 4.86, (3.70, 5.07) (4.97, 5.12) (1.70, 2.68, 2.76) 2.00, (3.29, 2.80)	Gln632, Lys606, Ala585, Ser705, Leu584, Ile638, Pro798, Lys633, Leu606, Leu634.
10.	Loganin pentaacetate	-7.0	9	2.42, 2.23, 2.85, (1.85, 2.41) 2.03, (1.89, 3.41, 3.37)	Lys633, Lys633, Thr636 Lys606, His635
11	Methyl 2, 6-dihydroxy-4-quinolinecarboxylate	-.5.8	8	1.97, 3.40 (3.88, 2.05) (5.19, 2.04) (4.79, 2.64)	Thr636, Glu610 Lys606, His635, Ala585 Gln648.
12	Nobiletin	-6.2	10	3.59, (2.91, 2.72) 4.79, (4.09, 4.23) 4.94, 5.43, 3.72, 3.77	Glu700, His635, Lys633, Glu610, Lys606, Lys633, Phe615, Gln632, Ala585.
13	Prunus inhibitor b	-9.2	12	(2.36, 2.80, 3.02) (3.46, 4.52, 4.76) 2.01, (4.00, 3.67) 4.98 (3.27, 1.99)	Leu634, Lys633, Glu700, His635, Ala585, Lys606.
14	Sativanine B	-8.0	7	(4.49, 3.93, 5.10) (4.36, 4.91) 3.59, 4.11	His635, Lys633, Leu609, Phe615.
15	R) -Skyrin 2-xyloside	9.3	17	4.36, 5.26, (3.99, 3.99) (2.23, 2.52, 2.82) 3.03, 2.47, 2.34, (4.76, 4.96, 4.06, 4.76, 3.73, 3.89) 4.67.	Phe615, Leu634, Glu610, Thr636, His635, Gln648, Gln632, Lys633, Lys633.
16	Sparteine	-5.5	0	0	Leu634, Phe615
17	Vismione D	-8.0	11	4.15, (5.15, 2.51, 5.15, 4.27, 2.57) 3.57, 2.86, 2.47, 1.98, 3.93.	Ala585, Lys633, Glu700, Lys606, Thr, Leu634, Phe615
18	Licorice glycoside E	-9.3	18	2.40, 4.17, 2.26, 4.21, 4.02 (2.41, 1.93, 2.49, 2.52) 3.26, 2.86, (3.68, 3.77) (4.15, 4.82, 3.90, 4.20) 2.26	Trp698, Pro798, Glu, Lys606, Ala585, Lys633, His635, Glu610.

Table 3 — Standard criteria of Molecular dynamics simulation of protein ligand complex

Complex Name	No. of Atoms in Systems (Protein + Ligand)	Box Volume (n/m^3)	Density of System (g/l)	No. of Solvent molecules added	Ions added	Fmax Steps
Dihydrocelastrol + 1DQA	6139	845.43	995.69	25549	$1Cl^-$	1656
Atorvastatin + 1DQA	6349	1048.43	991.19	32054	Nil	1599

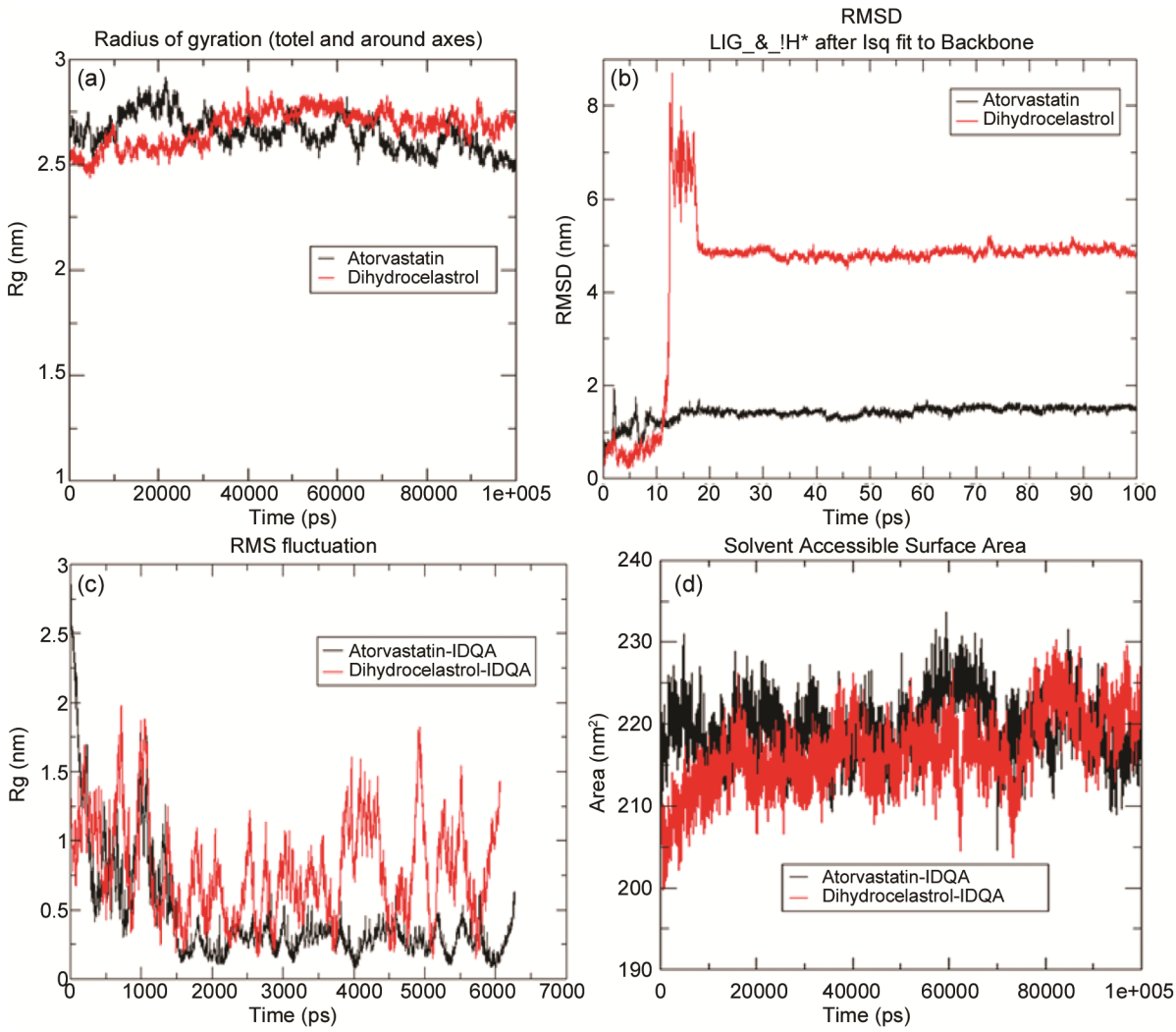

Fig. 5 — Molecular dynamics simulation (100 ns) results of protein HMG Co–A Reductase (1DQA) with dihydrocelastrol and atorvastatin complexes. (A) Radius of gyration; (B) Root Mean Square Deviation (RMSD); (C) Root Mean Square fluctuation (RMSF); and (D) Solvent Accessible Surface Area (SASA)

EEL, EPB, ENPOLAR, and EDISPER were all noted along with the complexes' GGAS, GSOLV, and GTOTAL values. The GGAS, GSOLV, and GTOTAL values for both the complexes were found significant where the eigen value gets stable at value 10 and remains stable till the end of calculations in both the complexes (Table 4).

Principal component analysis (PCA) was deployed to minimize the MD data dimensionality and to characterize protein-cavity fluctuations. PCA 1 of dihydrocelastrol + 1DQA complex shows RMSF up to 0.08Å and for Atorvastatin + 1DQA complex it comes under 0.1 Å, which is highly acceptable (Fig. 6). There are distinct groupings of conformations along the PC1 plane, PC2 plane, and PC3 plane. The interactive residue positions of dihydrocelastrol and atorvastatin with HMG-CoA reductase showed significant overlapping as indicated by black and blue lines (Fig. 7).

Table 4 — MMPSA calculation of free energy for Protein ligand complex

S. N	Complex	ΔGGAS (Kcal/mol)	ΔGSOLV (Kcal/mol)	ΔGTOTAL (Kcal/mol)
1	Dihydrocelastrol + 1DQA	-34.07	38.32	4.24
2	Atorvastatin + 1DQA	-38.10	44.49	6.39

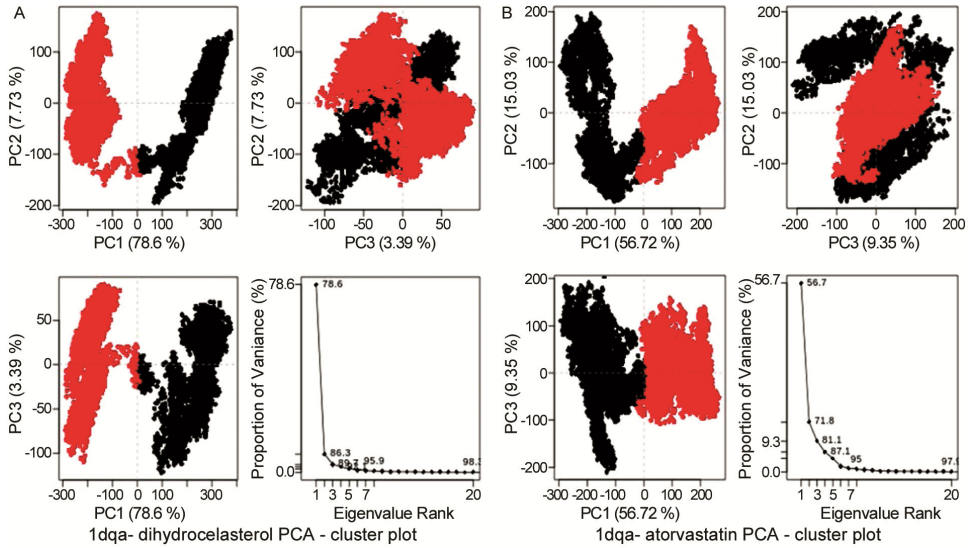

Fig. 6 — Cluster plot analysis of PCA (Principal Component Analysis) of dihydrocelastrol and atorvastatin against HMG Co-A reductase.

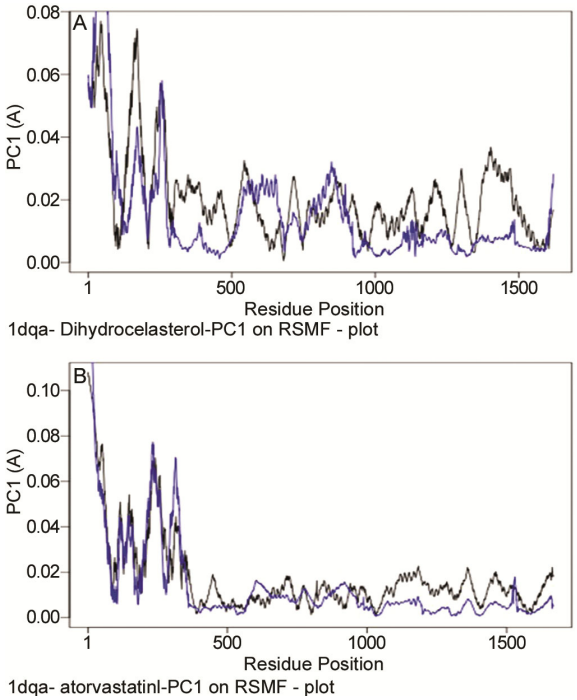

Fig. 7 — The interactive residue positions of Principal Component Analysis of dihydrocelastrol and atorvastatin with HMG-CoA reductase

Druggability assessment of ADMET prediction

The phytocompounds dihydrocelastrol, sparteine, and hecogenin follow the Lipinski rule of five and can cross the human intestinal barrier (HIA) as well as the blood-brain barrier (BBB) along with the gastrointestinal absorption as indicated by BOILED egg prediction. Vismione D and Methyl 2, 6-dihydroxy-4-quinolinecarboxylate were shown in the white part that indicates it has good potential to cross the HIA but were not able to cross BBB as the same result shown with the positive control such as atorvastatin indicated an ideal drug profile (Table 5).

Discussion

Plant extracts are a plethora of bioactive phytocompounds that possess potential to ameliorate several diseases via the established mechanisms and are novel sources for new drug discovery. The conventional medicines are formulations of the bioactive phytocompounds that have been practiced for a long time by numerous practitioners[33,34]. In this study, the assessment of the test extract showed the presence of 18 unique bioactive phytocompounds. The phytocompound identified possess bioactive potential and has been used for therapeutics of hypercholesterolemia. Accordingly, the dihydrocelastrol showed significant interaction with HMGCR (HMG-CoA reductase) as revealed by binding energy-8.9 kcal/mol. The interactions were followed by two significant dealings, *i.e.* specificity, which differentiates the highly specific binding partner from less specific associates, and affinity, which governs that a high attention of weakly interacting partners cannot

Table 5 — Physiochemical ADMET analysis of the leading phytocompounds aqueous extract of *Calligonum polygonoides* L. by SwissADME web tool

SN	Compound	MW g/mol	Log P	cLogP	HBA	HBD	nHB	TPSA	DEUGLIKENESS	Filter L/B
1	5, 4'-Dihydroxy-6-C-prenylflavanone 4'-xylosyl- (1->2) -rhamnoside	602.63	3.58	1.35	12	6	18	184.60 Å		-
2	12Z, 15S, 18S) -15-hydroxy-18-bromo-12, 16, 17-octadecatrienoic acid	373.33	3.49	4.64	3	2	5	57.53Å		B
3	Convallagenin B	464.63	3.72	2.86	6	4	10	99.38Å		-
4	D-Glucuronic acid 1-phosphate	2.74.12	-0.96	-0.96	10	6	16	183.79Å	Yes	L
5	Dihydrocelastrol	452.63	3.42	5.69	4	3	7	77.76Å		-
6	Hecogenin	430.62	4.06	4.39	4	1	5	55.76Å	Yes	L/B
7	Indican	295.29	1.96	-0.16	6	5	11	115.17Å		-
8	Khelloside	408.36	1.92	-0.11	10	4	14	151.96Å	Yes	L
9	Linoside B	639.60	3.08	-0.24	15	7	22	227.20Å		-
10	Loggnin pentaacetate	600.57	4.08	1.29	15	0	5	185.49Å		-
11	Methyl 2, 6-dihydroxy-4-quinolinecarboxylate	219.19	1.51	1.20	4	2	6	79.39Å	Yes	L
12	Nobiletin	402.399	3.96	3.02	8	0	8	85.59Å	Yes	L
13	Prunus inhibitor	560.5	2.09	1.99	11	8	19	189.53Å		-
14	Sativanine B	518.65	3.80	3.09	5	2	7	90.98Å	Yes	L
15	Skyrin 2 glycosidase	670.57	2.52	1.85	14	8	22	248.58Å		-
16	Sparteine	234.38	3.12	2.37	2	0	2	6.48Å	Yes	L/B
17	Vismione D	410.50	4.24	4.65	5	3	8	86.99Å	Yes	L
18	Licorice glycosidase	6.93.65	2.74	0.89	14	7	21	226.69Å		-

MW = molecular weight; iLogP= partition coefficient; ClogP = consensus log P; HBA= hydrogen bond acceptor; HBD= hydrogen bond donor; nHB= number of hydrogen bond; TPSA= total polar surface area; n violations = number of violations; Filter L= Lipinski rule of five and B= blood brain barrier

replace the effect of a low concentration of the detailed partner interacting with high affinity. Further assessments of complex topography were undertaken through molecular dynamic simulations which revealed significant stability and interaction strategies. The atorvastatin complex equilibrates faster as compared to the dihydrocelastrol complex. This shows that 1DQ protein was faster stabilized when it binds with Atorvastatin as compared to that of dihydrocelastrol. The RMSD of Atorvastatin remains lesser as compared to dihydrocelastrol, this shows the stability of atorvastatin over dihydrocelastrol as revealed by previous studies. Similarly, RMSD values resembled the values of RMSD which validates the complex's stabilities. RMSD represents a standard determination of the structural distance between coordinates whereas the RMSF is the standard deviation of a particle across from a reference position[29]. The SASA values of atorvastatin systems remain high over the dihydrocelastrol system which shows that in the Atorvastatin system protein is more available for the ligand. The lesser Coul-SR (Coul-SR (Coulombic short-range) and LJ-SR (Lennard-Jones short-range) values of dihydrocelastrol complexes indicate that dihydrocelastrol interacts better as compared to atorvastatin. It seems that there are significant interactions between the protein and ligand as resembled with values of peptide bonds, H bonds, and other covalent bonds. MMPBSA assessments revealed the sum of GGAS and GSOLV to GTOTAL values. Dihydrocelastrol complex shows lesser GTOTAL values as compared to Sitagliptin complexes. MMPBSA calculations showed significant considerations of interactions between ligands and receptors as revealed by minimum values of free energies. PCA reduces the dimensionality of large data sets with the minimum possible loss of information. The percentage of the total mean square displacement (or variance) of atom positional fluctuations captured in each dimension is

characterized by their corresponding eigen value. Here Eigen value gets stable at value 10 and remains stable till the end of calculations in both complexes. It is found that 3–5 dimensions are often sufficient to capture over 70% of the total variance in each family of structures. Thus, a handful of principal components are sufficient to provide a useful description while still retaining most of the variance in the original distribution.

Consequently, interactions of catalytic regions with ligands or phytocompounds limit the activity of enzymes or the capability of inhibition of specific enzymes or target proteins as per the different degrees of free energies which resemble significantly the results of *in vitro* inhibition assay. Furthermore, a high-fat diet and excess cholesterol with the administration of poloxamer 407 (P407) resulted in elevated peripheral cholesterol due to promoted cholesterol biosynthesis and unpackaged cholesterol in circulation. It has been illustrated that the mechanism of P407-encourage dhypercholesterolemia implicates raised triglyceride levels ensuing from the inhibition of lipoprotein lipase (LPL), and indirect encouragement of HMGCR through decreased LDL receptor expression in the liver[13,14]. Subsequently, LDL cholesterol, VLDL cholesterol, and triglyceride were significantly increased in the hypercholesterolemic animal model which indicates the improper packaging and recirculation of excess cholesterol. Whereas the treatment of the test extract and atorvastatin caused significant ameliorations in total cholesterol, LDL cholesterol, VLDL cholesterol, and triglyceride which indicated the interferences of bioactive phytocompounds by subsiding the cholesterol biosynthesis and packing of the different fractions of cholesterol as shown resemblance with several previous studies. Supportively, the packaging and reabsorption of the cholesterol improved by the treatments as revealed by the indices of the Castelli – I, Castelli- II, atherogenic coefficient, and atherogenic index of plasma (AIP). Consequently, hypercholesterolemia is a metabolic disorder disease associated with the behavior of high-fat diet consumption, directing to high cholesterol in vessels which triggers oxidative stress and diminishes antioxidant competence. Oxidative stress is an unevenness between the production of free radicals and the antioxidative system, resulting in damage to DNA, protein, and fat by the lipid peroxidation process. These kinds of degenerative changes such as necrosis, pyknosis, and apoptosis were shown in the intima and subsequent layers of the vascular wall with the inflammatory changes and accumulation of foam cells. The treatment of the test extract caused significant ameliorations and scavenging of the free radicals by making significant alterations in GSH, LPO, and FRAP values. These kinds of alterations may follow freeradical scavenging capabilities of the potent bioactive phytocompounds as reported by several studies. The treatments of the test extract and atorvastatin caused significant reductions in the accumulated bulging area of fatty substances which may be reduced through interferences of exhibited bioactive phytocompounds by inhibition of target enzyme of HMGCR, reducing the free radicals and linked mechanisms as reported by severall and marked studies. The potent bioactive phytocompound *i.e.*, dihydrocelastrol and other exhibited phytoconstituents of the test extract following the five rules of the Lipinski (MW, iLOGP, HBAs, and HBDs), as well as four other parameters such as molecular polar surface area (TPSA), number of rotatable bonds (ROTBs), number of aromatic rings (nAROMs) which revealed the druggability.

Conclusion

It can be concluded that aqueous shoot extract of the *Calligonum polygonoides* L. possesses potent bioactive phytocompounds that have significant hypocholesterolemic potential through inhibition of HMG-CoA reductase (HMGCR), along with scavenging capabilities of free radicals which reduces the oxidative stress. It appears that the phytocompounds such as dihydrocelastrol significantly interact with HMGCR as per the assessments of *in vitro* inhibition assay, molecular docking, and molecular dynamics simulation resulted to subside the cholesterol biosynthesis. The reduced oxidative stress and subsided cholesterol biosynthesis caused significant alterations in the histopathology of atherosclerotic plaque.

Acknowledgement

All authors declare no conflict of interest. The animal protocol (IAEC No: JNVU/IAEC/2020/02) was approved and recommended by the IAEC (Institutional Animal Ethical Committee).

Conflict of interests

All authors declare no conflict of interests.

References

1 Sudhakaran S, Bottiglieri T, Tecson KM, Kluger AY & McCullough PA, Alteration of lipid metabolism in chronic kidney disease, the role of novel antihyperlipidemic agents, and future directions. *Rev Cardiovasc Med*, 19 (2018) 77.

2 Orozco MF, Vázquez-Hernández A & Fenton-Navarro B, Active compounds of medicinal plants, mechanism for antioxidant and beneficial effects. *Phyton*, 88 (2019) 1.

3 Aldesuquy H & Abdelaal M, Phytochemical Constituents, Antibacterial and Antioxidant Activities of some Medicinal Plants. *Curr Trends Biomed Eng Biosci*, 16 (2018).

4 Kaikini AA, Dhande SR & Kadam VJ. Antihyperlipidemic activity of methanolic extract of leaves of Bambusa bambos Druce against poloxamer-407 induced hyperlipidemia in rats. *Int J Pharm Pharm Sci,* 7 (2014) 393.

5 Keskes H, Belhadj S, Jlail L, El Feki A, Damak M, Sayadi S & Allouche N, LC-MS-MS and GC-MS analyses of biologically active extracts and fractions from Tunisian Juniperus phoenicea leaves. *Pharm Biol,* 55 (2017) 88.

6 Zhu ZJ, Schultz AW, Wang J, Johnson CH, Yannone SM, Patti GJ & Siuzdak Gary, Liquid chromatography quadrupole time-of-flight mass spectrometry characterization of metabolites guided by the METLIN database. *Nat Protoc,* 8 (2013) 451.

7 Schointuch MN, Gilliam TP, Stine JE, Han X, Zhou C, Gehrig PA, Kim K & Jump BLV, Simvastatin, an HMG-CoA reductase inhibitor, exhibits anti-metastatic and anti-tumorigenic effects in endometrial cancer. *Gynecol Oncol,* 134 (2014) 346.

8 Hafidz K, Puspitasari N, Azminah A, Yanuar A, Artha Y & Mun'im A, HMG-CoA reductase inhibitory activity of Gnetumgnemon seed extract and identification of potential inhibitors for lowering cholesterol level. *J Young Pharm,* 9 (2017) 559.

9 Johnston TP, The P-407–induced murine model of dose-controlled hyperlipidemia and atherosclerosis: a review of findings to date. *J Cardiovasc Pharmacol,* 43 (2004) 595.

10 Kim M, Kim TW, Kim CJ, Shin MS, Hong M, Park HS & Park SS, Berberine ameliorates brain inflammation in poloxamer 407-induced hyperlipidemic rats. *Int Neurourol J,* 23 (2019) S102.

11 Palmer WK, Emeson EE & Johnston TP, The poloxamer 407-induced hyperlipidemic atherogenic animal model. *Med Sci Sports Exerc*, 29 (1997) 1416.

12 Ohkawa H, Ohishi N & Yagi K, Assay for lipid peroxides in animal tissues by thiobarbituric acid reaction. *Anal Biochem,* 95 (1979) 351.

13 Weydert CJ & Cullen JJ, Measurement of superoxide dismutase, catalase and glutathione peroxidase in cultured cells and tissue. *Nat Protoc,* 5 (2010) 51.

14 Griffin S & Bhagooli R, Measuring antioxidant potential in corals using the FRAP assay. *J Exp Mar Biol Ecol*, 302 (2004) 201.

15 Thaipong K, Boonprakob U, Crosby K, Cisneros-Zevallos L & Byrne D, Comparison of ABTS, DPPH, FRAP, and ORAC assays for estimating antioxidant activity from guava fruit extracts. *J Food Compos Anal*, 19 (2006) 669.

16 Forli S, Huey R, Pique ME, Sanner MF, Goodsell DS & Olson AJ, Computational protein-ligand docking and virtual drug screening with the AutoDock suite. *Nat Protoc*, 11 (2016) 905.

17 Ahmed H, Moawad A, Owis A, AbouZid S & Ahmed O. Flavonoids of *Calligonum polygonoides* and their cytotoxicity. *Pharm Biol,* 54 (2016) 2119.

18 Alazmi M & Motwalli O, *In silico* virtual screening, characterization, docking and molecular dynamics studies of crucial SARS-CoV-2 proteins. *J Biomol Struct Dyn*, 39 (2021) 6761.

19 Lipinski CA, Lombardo F, Dominy BW & Feeney PJ, Experimental and computational approaches to estimate solubility and permeability in drug discovery and development settings. *Adv Drug Deliv Rev*, 23 (1997) 3.

20 Ghose AK, Viswanadhan VN & Wendoloski JJ, A knowledge-based approach in designing combinatorial or medicinal chemistry libraries for drug discovery. 1. A qualitative and quantitative characterization of known drug databases. *J Comb Chem*, 1 (1999) 55.

21 Chen J, Lee SK, Abd-Elgaliel WR, Liang L, Galende EY, Hajjar RJ & Tung CH, Assessment of cardiovascular fibrosis using novel fluorescent probes. *PLoS One,* 6 (2011) e19097.

22 Steck TL & Lange Y. Cell cholesterol homeostasis: mediation by active cholesterol. *Trends Cell Biol*, 20 (2010) 680.

23 Willey JZ & Elkind MS, 3-Hydroxy-3-methylglutaryl-coenzyme A reductase inhibitors in the treatment of central nervous system diseases. *Arch Neurol,* 67 (2010) 1062.

24 Koleva DI, Andreeva-Gateva PA, Orbetzova M, Atanassova I & Nikolova J, Atherogenic index of plasma, Castelli risk indexes and leptin/adiponectin ratio in women with metabolic syndrome. *Int J Pharm Med Res,* 3 (2015) 12.

25 Charan J, Riyad P, Ram H, Purohit A, Ambwani S, Kashyap P, Singh G, Hashem A, Allah, EFA, Gupta VK, Kumar A & Panwar A, Ameliorations in dyslipidemia and atherosclerotic plaque by the inhibition of HMG-CoA reductase and antioxidant potential of phytoconstituents of an aqueous seed extract of *Acacia senegal* (L.) Willd in rabbits. *PLoS One,* 17 (2022) e0264646.

26 Chapple IL, Role of free radicals and antioxidants in the pathogenesis of the inflammatory periodontal diseases. *Clin Mol Pathol,* 49 (1996) M247.

27 Rahman K, Studies on free radicals, antioxidants, and co-factors. *Clin Interv Aging*, 2 (2007) 219.

28 Lee KJ, Woo ER, Choi CY, Shin DW, Lee DG, You HJ & Jeong HG, Protective effect of acteoside on carbon tetrachloride-induced hepatotoxicity. *Life Sci,* 74 (2004) 1051.

29 Zhu Y, Liu F, Zou X & Torbey M, Comparison of unbiased estimation of neuronal number in the rat hippocampus with different staining methods. *J Neurosci Methods,* 254 (2015) 73.

30 Burgess N, Maguire EA & O'Keefe J, The human hippocampus and spatial and episodic memory. *Neuron,* 35 (2002) 625.

31 Sobesky JL, Barrientos RM, Henning S, Thompson BM, Weber MD, Watkins LR & Maier SF, High-fat diet consumption disrupts memory and primes elevations in hippocampal IL-1β, an effect that can be prevented with dietary reversal or IL-1 receptor antagonism. *Brain Behav Immun*, 42 (2014) 22.

32 Bhutada P, Mundhada Y, Bansod K, Tawari S, Patil S, Dixit P, Umathe S & Mundhada D, Protection of cholinergic and antioxidant system contributes to the effect of berberine ameliorating memory dysfunction in a rat model of streptozotocin-induced diabetes. *Behav Brain Res,* 220 (2011) 30.

33 Innih SO, Eze IG & Omage K, Cardiovascular benefits of *Momordica charantia* in cholesterol-fed Wistar rats. *Clin Phytosci,* 7 (2021) 1.

34 Watanabe TK, Suzuki M, Yamasaki Y, Okuno S, Hishigaki H, Ono T, Oga K, Mizoguchi-Miyakita A, Tsuji A, Kanemoto N, Wakitani S, Takagi T, Nakamura Y & Tanigami A, Mutated G-protein-coupled receptor GPR10 is responsible for the hyperphagia/dyslipidemia/obesity locus of Dmo1 in the OLETF rat. *Clin Exp Pharmacol Physiol*, 32 (2005) 355.